Although we did not yet succeed in interpreting the details of the motions which take place in the other phases several general conclusions can already be drawn. In particular it appears that the solid-solid transitions are accompanied by discontinuous changes in the dynamic state of the side chains and that these changes involve in each case all the methylene carbons. This is in contrast to the interference based on the thermodynamic data which were interpreted in terms of stepwise melting of the side chains,[4] starting at the end methyl group. It is clear that these changes in the dynamic state of the side chain must be accompanied by changes in the molecular packing and of the crystal structure during the respective phase transitions. Such data are however not yet available for BHA6 in its various phases.

Acknowledgment. This research was supported by the United States–Israel Binational Science Foundation, Jerusalem. E.L. is a recipient of a Sir Charles Clore Post-Doctoral Fellowship.

Registry No. BHA6, 65201-69-6; BHA6-*2-d*, 110473-71-7; BHA6-*3-d*, 110473-72-8; BHA6-*4-d*, 110473-73-9; BHA6-*5-d*, 110473-74-0; BHA6-*6-d*, 110473-75-1.

Reduction of the Binuclear Iron Site in Octameric Methemerythrins. Characterizations of Intermediates and a Unifying Reaction Scheme

Linda L. Pearce,[†] Donald M. Kurtz, Jr.,*[†] Yao-Min Xia,[‡] and Peter G. Debrunner[‡]

Contribution from the Department of Chemistry, Iowa State University, Ames, Iowa 50011, and Department of Physics, University of Illinois, Urbana, Illinois 61801.
Received December 17, 1986

Abstract: Three oxidation levels are observed during reduction of the binuclear iron site in hemerythrin (Hr), namely, met [Fe(III),Fe(III)], semi-met [Fe(II),Fe(III)], and deoxy [Fe(II),Fe(II)]. Using absorption, EPR, and Mössbauer spectroscopies, we have characterized the two kinetically identifiable intermediates observed during the three stages of reduction of met- to deoxyHr. Our results establish for the first time the following characteristics about reduction of the iron sites in octameric metHr's by inorganic reducing agents between pH 6.3 and 8.2: (i) The latter two stages of reduction of *Phascolopsis gouldii* metHr have rate constants very similar to those previously published for *Themiste zostericola* Hr; these rate constants are independent of both concentration and nature of the reducing agent. (ii) The extent of antiferromagnetic coupling in the first-stage product, $(\text{semi-met})_R\text{Hr}$, is ~5 times lower than that in metHr. (iii) The second-stage product consists of a mixture of deoxy and met oxidation levels; the latter we label met′ because of its inability to bind N_3^- and its unusual Mössbauer parameters. (iv) When an excess of reductant is used, ~70% of the iron sites in the second-stage product is at the deoxy level. (v) There are no detectable effects of D_2O on the rates of reduction. From these characterizations we propose a scheme for reduction of the iron site in Hr that unifies our results with those from several previous studies. A novel premise implied by our scheme is that only the iron atom closer to the outer surface of each subunit in the octamer is reduced by "outer-sphere" reagents. Thus, the product of the first stage of reduction, $(\text{semi-met})_R\text{Hr}$, has this outer iron atom reduced. Reduction beyond the semi-met level requires electron exchange within the binuclear iron site such that the outer iron atom becomes reoxidized. A conformational change, during which this electron exchange occurs, is proposed to be the rate-determining step for the second stage. Relatively rapid reduction to deoxy can then occur directly either by the inorganic reagent or by disproportionation. Thus, these latter two processes are both conformationally controlled. According to our scheme, the proportions of met′ and deoxy in the second-stage product are determined by the relative rates of direct reduction vs disproportionation. The third stage we propose consists of rate-determining conversion of met′Hr back to metHr, after which normal reduction kinetics resume. The proposed scheme appears to be applicable to reduction of the iron site in monomeric metmyoHr as well. Our results provide a context for understanding reduction of the iron site in Hr by the apparent physiological reducing agent, cytochrome b_5.

Hemerythrin (Hr) is a respiratory protein found in several phyla of marine invertebrates. The protein from most species consists of an octamer of essentially identical subunits, each of which contains a binuclear non-heme iron oxygen-binding site.[1] A variety of physical studies, including X-ray crystallography,[2] and comparisons to synthetic complexes[3-5] have given a clear picture of the structural and electronic properties of this unique site. The structure of the iron site in [Fe(III),Fe(III)]metHr that has emerged from these studies has one six-coordinate iron atom, Fe1, and one five-coordinate iron atom, Fe2. The two iron atoms are linked to the protein by terminal imidazole and bridging carboxylate ligands. A third bridging ligand is provided by solvent in the form of an oxo ion. The presence of the μ-oxo bridge mediates a high degree of antiferromagnetic coupling between the high-spin ferric ions in metHr ($J = -134$ cm^{-1}), and this coupling is largely conserved in oxyHr.[6,7] The vacant site on Fe2

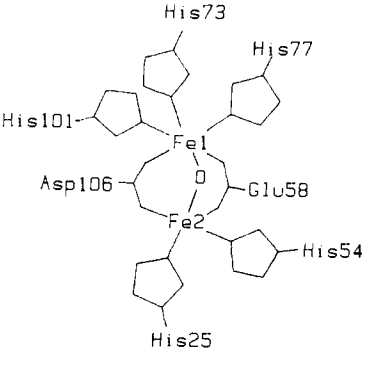

*Present address: Department of Chemistry, University of Georgia, Athens, GA 30602.
[†]Iowa State University.
[‡]University of Illinois.

(1) Klotz, I. M.; Kurtz, D. M., Jr. *Acc. Chem. Res.* **1984**, *17*, 17-22.

0002-7863/87/1509-7286$01.50/0

is occupied by hydroperoxide, OOH^-, in oxyHr[8] and by any of a number of anions, X^-, in metHrX adducts. Particularly stable adducts of metHr are formed with N_3^- and, at pH $\gtrsim$8, with OH^-.[9] A smaller degree of antiferromagnetic coupling in [Fe(II),Fe(III)]semi-metHrX adducts and in [Fe(II),Fe(II)]deoxyHr has been attributed to protonation of the μ-oxo bridge between the iron atoms, with essential retention of the remaining structural features shown above.[7,8,10] The antiferromagnetic coupling leads to ground spin states $S = 0$ for oxy-, deoxy-, and metHrs and $S = {}^1/_2$ for semi-metHr.

Interconversions between the various oxidation levels of the iron site, summarized below, have been the subjects of several kinetic studies with inorganic redox agents.[11-15]

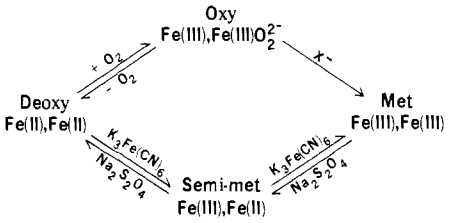

These studies have established inter alia that one-electron reduction of metHr yields $(semi\text{-}met)_R$Hr, a form that differs in spectroscopy and reactivity from $(semi\text{-}met)_O$Hr, produced by one-electron oxidation of deoxyHr.[11,16] While the exact nature of the difference between $(semi\text{-}met)_O$ and $(semi\text{-}met)_R$ has not been established, a small difference in rhombic distortion of the ferrous site is apparently sufficient to account for the differences in the EPR spectra of these two forms.[17]

Our interest in redox interconversions of the iron site in Hr stems from the discovery in this laboratory of a metHr reduction system in erythrocytes of the sipunculan worm, *Phascolopsis gouldii*.[18] In this system the primary electron donor to metHr is cytochrome b_5, which is presumably present to counteract the autoxidation of oxy- to metHr.[11] Despite fairly intensive study, some aspects of the mechanism of reduction of met- to deoxyHr by inorganic reagents have remained elusive. Three stages in the kinetics of reduction of metHr from *P. gouldii* were first observed by Harrington et al.[19] and later for metHr from *Themiste zostericola* by Armstrong et al.[13] However, the identity of the second-stage product has been a point of contention.[13,14] Using a variety of approaches, we have characterized the kinetically identifiable intermediates between met- and deoxyHr in a more thorough manner than in any previous study. From these characterizations we propose a scheme that unifies results from several previous studies and, in addition, provides a context within which reduction of metHr by the physiological system can be understood.

Experimental Section

Preparation of MetHr. Live worms of the species *P. gouldii* were obtained from the Marine Biological Laboratory, Woods Hole, MA. Crystalline oxyHr was obtained by a standard procedure.[20] The crystalline protein was dissolved in 50 mM Tris–acetate, pH 8.0, containing 150 mM Na_2SO_4. The solution of oxyHr was then dialyzed at 4 °C against 3–4 mM $K_3Fe(CN)_6$. Alternatively, solid $K_3Fe(CN)_6$ was added directly to the protein solution and allowed to react for several hours at room temperature. Excess reagent was removed by *extensive* dialysis at 4 °C. MetHr thus obtained was dialyzed against 50 mM HEPES, MES, or EPPS[21] buffers containing 150 mM Na_2SO_4. The pHs of these buffers were adjusted with NaOH. Concentrations of metHr were determined by addition of sodium azide and the use of $\epsilon_{446} = 3700\ M^{-1}\ cm^{-1}$ for $metHrN_3$.[22] Concentrations are expressed in terms of subunits, i.e., binuclear iron sites. Live worms of the species *Themiste zostericola* were obtained from Pacific Biomarine Supply, Venice, CA. OxyHr was prepared as previously described[20] except that the crystallization step was omitted. MetHr from *T. zostericola* was prepared in the same manner as described above for Hr from *P. gouldii*.

Solutions of metHr in D_2O were prepared by dialyzing ~1 mL of a solution of metHr in buffered H_2O against ~100 mL of buffered D_2O for ~24 h at 4 °C. The pD was determined by using the equation pD = pH meter reading + 0.4. A Beckman Model 31 pH meter was used for the measurements.

Preparation of Reducing Agents. $Cr(H_2O)_6^{2+}$ was obtained by oxidation of Cr metal. Chromium metal, obtained from Aldrich Chemical Co., was ~100 mesh and 99.9% pure. Approximately 100 mg of Cr metal was placed under a N_2 atmosphere, and ~0.5 mL of concentrated HCl was added to start the reaction. The Cr metal was then washed with 0.25 M $HClO_4$ several times, and 3–4 mL of 0.25 M $HClO_4$ was added. $[Cr(H_2O)_6](ClO_4)_2$ was produced over a period of 30–45 min. The reaction was allowed to proceed until no further H_2 evolution was observed. Unreacted Cr metal was removed by filtration through a Schlenkware frit. The concentration of $[Cr(H_2O)_6](ClO_4)_2$ was determined spectrophotometrically with $\epsilon_{750} = 4.38\ M^{-1}\ cm^{-1}$.[23] When used for reductions of metHr, these solutions of $[Cr(H_2O)_6]^{2+}$ were diluted with 0.1 M sodium cacodylate (pH 7.0). Concentrations of Cr^{2+} in the solutions containing cacodylate were determined by anaerobic titration with $KMnO_4$.[24a]

$[Cr(15\text{-}aneN_4)(H_2O)_2]^{2+}$ was prepared under N_2 by slow addition of $[Cr(H_2O)_6](ClO_4)_2$ (prepared as described above) to a 2-fold molar excess of 15-$aneN_4$[21] (Strem Chemicals, Inc.) in 50 mM MES, HEPES, or EPPS at the desired pH. Concentrations of $[Cr(15\text{-}aneN_4)(H_2O)_2]^{2+}$ were determined spectrophotometrically with $\epsilon_{540} = 36.5\ M^{-1}\ cm^{-1}$.[25] $[Cr(15\text{-}aneN_4)(D_2O)_2]^{2+}$ in ~90% D_2O was prepared by addition of $[Cr(H_2O)_6]ClO_4)$ to a buffered solution of 15-$aneN_4$ in D_2O.

$Na_2S_2O_4$ was obtained from BDH Chemicals, Ltd., Poole, England, and used without further purification. Concentrations of stock solutions of $Na_2S_2O_4$ were determined by titration with solutions of $K_3Fe(CN)_6$, whose concentrations were determined with $\epsilon_{420} = 1030\ M^{-1}\ cm^{-1}$.[26] $Fe(EDTA)^{2-}$ was prepared according to the method of Wherland et al.[27] in buffered H_2O and buffered D_2O solutions.

(2) Stenkamp, R. E.; Sieker, L. C.; Jensen, L. H. *J. Am. Chem. Soc.* **1984**, *106*, 618–622. Sieker, L. C.; Stenkamp, R. E.; Jensen, L. H. In *The Biological Chemistry of Iron*; Dunford, H. B., Dolphin, D., Raymond, K. N., Sieker, L., Eds.; Reidel: New York, 1982; pp 161–175.
(3) Armstrong, W. H.; Spool, A.; Papaefthymiou, G. C.; Frankel, R. B.; Lippard, S. J. *J. Am. Chem. Soc.* **1984**, *106*, 3653–3667.
(4) Armstrong, W. H.; Lippard, S. J. *J. Am. Chem. Soc.* **1984**, *106*, 4632–4633.
(5) Chauduri, P.; Wieghardt, K.; Nuber, B.; Weiss, J. *Angew. Chem., Int. Ed. Engl.* **1985**, *24*, 778–779.
(6) Dawson, J. W.; Gray, H. B.; Hoenig, H. E.; Rossman, G. R.; Schredder, J. M.; Wang, R. H. *Biochemistry* **1972**, *11*, 461–465.
(7) Maroney, M. J.; Kurtz, D. M., Jr.; Nocek, J. M.; Pearce, L. L.; Que, L., Jr. *J. Am. Chem. Soc.* **1986**, *108*, 6871–6879.
(8) Stenkamp, R. E.; Sieker, L. C.; Jensen, L. H.; McCallum, J. D.; Sanders-Loehr, J. *Proc. Natl. Acad. Sci. U.S.A.* **1985**, *82*, 713–716.
(9) Shiemke, A. K.; Loehr, T. M.; Sanders-Loehr, J. *J. Am. Chem. Soc.* **1986**, *108*, 2437–2443.
(10) Reem, R. C.; Solomon, E. I. *J. Am. Chem. Soc.* **1987**, *109*, 1216–1226.
(11) Wilkins, R. G.; Harrington, P. C. *Adv. Inorg. Biochem.* **1983**, *5*, 51–85, and references therein.
(12) Nocek, J. M.; Kurtz, D. M., Jr.; Pickering, R. A.; Doyle, M. P. *J. Biol. Chem.* **1984**, *259*, 12334–12338.
(13) Armstrong, G. D.; Ramasami, T.; Sykes, A. G. *Inorg. Chem.* **1985**, *24*, 3230–3234.
(14) Bradič, Z.; Tsukahara, K.; Wilkins, P. C.; Wilkins, R. G. In *Frontiers of Bioinorganic Chemistry*; Xavier, A. V., Ed.; VCH: Weinheim, FRG, 1986; pp 336–344.
(15) Armstrong, G. D.; Sykes, A. G. *Inorg. Chem.* **1986**, *25*, 3514–3516.
(16) Muhoberac, B. B.; Wharton, D. C.; Babcock, L. M.; Harrington, P. C.; Wilkins, R. G. *Biochim. Biophys. Acta* **1980**, *626*, 337–345.
(17) Bertrand, P.; Guigliarelli, B.; Gayda, J. P. *Arch. Biochem. Biophys.* **1986**, *245*, 305–307.
(18) Utecht, R. E.; Kurtz, D. M., Jr. *Inorg. Chem.* **1985**, *24*, 4458–4459.
(19) Harrington, P. C.; deWaal, D. J.-A.; Wilkins, R. G. *Arch. Biochem. Biophys.* **1978**, *191*, 444–451.
(20) Klotz, I. M.; Klotz, T. A.; Fiess, H. A. *Arch. Biochem. Biophys.* **1957**, *68*, 284–299.
(21) Abbreviations used: Tris, tris(hydroxymethyl)aminomethane; MES, 2-(*N*-morpholino)ethanesulfonate; HEPES, *N*-(2-hydroxyethyl)piperazine-*N*'-2-ethanesulfonate; EPPS, *N*-(2-hydroxyethyl)piperazine-*N*'-3-propanesulfonate; EDTA, ethylenediaminetetraacetate; 15-$aneN_4$, 1,4,8,12-tetraazacyclopentadecane.
(22) Garbett, K.; Darnall, D. W.; Klotz, I. M.; Williams, R. J. P. *Arch. Biochem. Biophys.* **1969**, *135*, 419–434.
(23) Tanabe, Y.; Sugano, S. *J. Phys. Soc. Jpn.* **1954**, *9*, 766–779.
(24) (a) Dawson, J. W.; Gray, H. B.; Holwerda, R. A.; Westhead, E. W. *Proc. Natl. Acad. Sci. U.S.A.* **1972**, *69*, 30–33. (b) Sandell, E. B. In *Colorimetric Determination of Traces of Metals*, 3rd ed.; Interscience: New York, 1959; pp 392–397.
(25) Adzamli, I. K.; Henderson, R. A.; Sinclair-Day, J. D.; Sykes, A. G. *Inorg. Chem.* **1984**, *23*, 3069–3073.
(26) Irwin, M. J.; Duff, L. L.; Shriver, D. F.; Klotz, I. M. *Arch. Biochem. Biophys.* **1983**, *224*, 473–478.
(27) Wherland, S.; Holwerda, R. A.; Rosenberg, R. C.; Gray, H. B. *J. Am. Chem. Soc.* **1975**, *97*, 5260–5262.

Collection and Analysis of Kinetic Data. A Perkin-Elmer Model 554 spectrophotometer was used to obtain kinetic data for reactions with $k_{obsd} \lesssim 0.1\ s^{-1}$. Reactions were monitored from 400 to 320 nm. Reactions on faster time scales were monitored by use of a stopped-flow device assembled in this laboratory. An Aminco-Morrow mixing chamber was installed in the optical path of a Beckman Model B spectrophotometer. Volumes of 1 mL of Hr and reductant solutions were anaerobically added to adjacent drive syringes. Absorbance traces were collected at fixed wavelengths between 400 and 380 nm and displayed on a Tektronix Model 5150 storage oscilloscope.

For spectrophotometric purposes, reactions were carried out under N_2 in a 1-cm-path semimicrocuvette. Trace O_2 was removed from N_2 with chromous scrubbing towers. Protein concentrations were maintained at 0.1 mM. Unless otherwise noted, all protein solutions contained 50 mM MES (pH 6.3), HEPES (pH 7.0), or EPPS (pH 8.2) and 150 mM Na_2SO_4. Reductant concentrations were varied from 1 to 5 mM with the exception of Cr^{2+}/cacodylate. Concentrations of Cr^{2+}/cacodylate higher than 2 mM caused precipitation of Hr. Reactions were also followed by addition of excess sodium azide at various times. Total reaction volume was 1.0 mL for reactions monitored by conventional spectrophotometry. Constant temperature (±0.1 °C) was maintained by a Brinkman constant-temperature bath connected to a thermostated cell holder or mixing chamber.

Rate constants were determined by fitting absorbance vs time data with the least-squares program EXPSUM, obtained from the laboratory of Professor J. H. Espenson. Rate constants reported are the average of three to five replicate determinations.

Chromium Binding to Hemerythrin. After reactions of Hr with Cr^{2+}(aq) or $[Cr(15\text{-ane}N_4)(H_2O)_2]^{2+}$ in HEPES at pH 7.0, selected solutions were analyzed to determine the amount of chromium bound to Hr. In order to remove excess reagent, the Hr solutions were either dialyzed or passed over a small Sephadex G-25 column. Concentrations of Cr were then determined by the diphenylcarbazide method,[24b] after transferring the Hr solutions to diluted H_2SO_4 and oxidizing with ammonium persulfate. Concentrations of Hr were determined as metHrN_3 prior to reactions with the chromous complexes. Analyses of undialyzed solutions of Hr corresponded to the total amount of chromous complex added. Analyses of solutions of metHr to which Cr^{3+} had been added shown no Cr after dialysis.

EPR Spectroscopy. Reactions monitored by EPR spectroscopy were carried out in septum-capped 2-dram vials under N_2 with the reagent and salt concentrations listed above. At various times 100-μL aliquots were transferred anaerobically with a gas-tight syringe to 4-mm-o.d. quartz tubes. The samples were then quickly frozen in a liquid-N_2 bath and the tubes flame-sealed under dynamic vacuum. EPR spectra were obtained on a Bruker Model ER-220D spectrometer equipped with an Oxford Instruments liquid-helium cryostat. When time courses of reactions were monitored, EPR instrument parameters were the following: frequency, 9.43 GHz; power, 0.2 mW; modulation, 16 G at 100 kHz; time constant, 0.1 s; gain, 1×10^{-5} to 1×10^{-3}. Spectra were collected at a fixed temperature between 4 and 12 K. Spin quantitations were achieved by double integration of areas of first-derivative spectra and use of copper sulfate as the concentration standard.[28]

For measurements of EPR power saturation vs temperature, *P. gouldii* metHr at a concentration of 2 mM was prepared in 50 mM MES (pH 6.3). $(Semi\text{-}met)_RHr$ was prepared from this solution by anaerobic addition of 1 equiv of $Na_2S_2O_4$. Semi-metHrN_3 was prepared in the same fashion with subsequent addition of excess NaN_3. (μ-S^{2-})Semi-metHr was prepared by anaerobic dialysis of the solution of metHr against sodium sulfide.[29] Samples of these solutions for EPR measurements were prepared as described above. Power saturation data were collected at temperatures ranging from 4.2 to 10 K by measuring the EPR absorption derivative signal intensity, I, as a function of incident microwave power, P. Signal intensities were measured at $g = 1.87$ (peak to peak) for $(semi\text{-}met)_RHr$, $g = 1.92$ for semi-metHrN_3, and $g = 1.87$ for (μ-S^{2-})semi-metHr. The data at each temperature were analyzed according to

$$\log (I/P^{1/2}) = a - (b/2) \log (P_{1/2} + P)$$

and the half-saturation power, $P_{1/2}$, was determined by a graphical method.[30]

Mössbauer Spectroscopy. Samples of metHrs from *T. zostericola* and *P. gouldii* at intermediate stages of reduction were prepared by anaerobic addition of either 1.5–2 equiv of $[Cr(15\text{-ane}N_4)(H_2O)_2]^{2+}$ per binuclear iron site or excess $Na_2S_2O_4$. The concentrations of Hr required for Mössbauer spectroscopy (5–8 mM) precluded the use of larger excesses of $[Cr(15\text{-ane}N_4)(H_2O)_2]^{2+}$. Samples were transferred anaerobically to 0.5-in.-diameter cylindrical nylon cups and frozen in a liquid-N_2 bath when no EPR signal was observable in samples made under comparable conditions. A sample of *T. zostericola* deoxyHr was prepared by anaerobic dialysis of metHr against $Na_2S_2O_4$ and transferred as described above. The Mössbauer samples contained ^{57}Fe in the natural isotopic abundance. ^{57}Fe Mössbauer spectra were obtained in the Department of Physics at the University of Illinois. The spectrometer was of the constant-acceleration type. Spectra were obtained at 100, 4, or 1.8 K with and without magnetic fields of up to 2.2 kG. Isomer shifts are quoted relative to iron metal at 300 K. The data were fitted with a sum of Lorentzians by using a least-squares routine.[31]

Table I. Rate Constants for Reduction of *P. gouldii* MetHr[a]

reducing agent	k_1, $M^{-1}\ s^{-1}$	$k_2 \times 10^3$, s^{-1}	$k_3 \times 10^4$, s^{-1}
Cr^{2+}/cacodylate[b]	34 (±4)	2.1 (±0.2)	1.7 (±0.3)
$[Cr(15\text{-ane}N_4)(H_2O)_2]^{2+}$	600 (±14)	3.7 (±0.2)	2.3 (±0.2)
$Na_2S_2O_4$	1.4 (±0.1) × 10^5	2.3 (±0.1)	1.7 (±0.2)

[a] 50 mM HEPES, pH 7.0, 20 °C, 150 mM Na_2SO_4. [b] 0.1 M sodium cacodylate, pH 7.0, 20 °C, 50 mM $NaClO_4$.

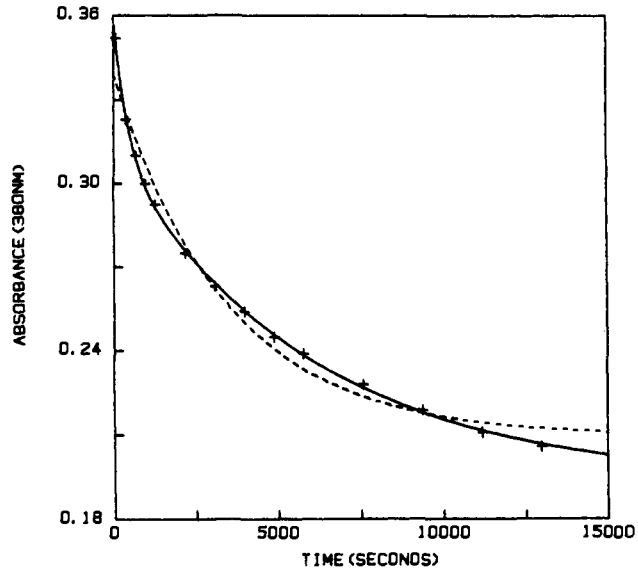

Figure 1. Nonlinear least-squares fits of the absorbance at 380 nm vs time data for reduction of 0.1 mM *P. gouldii* metHr by a 10-fold molar excess of $Na_2S_2O_4$ at pH 7.0 (50 mM HEPES), 150 mM Na_2SO_4, 20 °C. Key: (+) experimental absorbance vs time data; (---) fit using one exponential; (—) fit using two exponentials.

Results

Kinetics. The kinetics of reduction of octameric metHr from *T. zostericola*, as determined from absorbance changes, have been thoroughly examined recently,[13] whereas the physiological metHr reduction system is more thoroughly characterized in *P. gouldii*.[18] Therefore, in the present study, we have determined rate constants from absorbance changes during reduction of metHr only from *P. gouldii*.

Rate constants for reductions of metHr by excesses of Cr^{2+}/cacodylate, $[Cr(15\text{-ane}N_4)(H_2O)_2]^{2+}$, and $Na_2S_2O_4$ are reported in Table I. In each case we resolve three stages. The first stage is dependent on concentration of reductant, while the latter two are not. The latter two stages are also essentially independent of identity of reductant. Rate constant k_2 is only slightly dependent on pH. In the case of $[Cr(15\text{-ane}N_4)(H_2O)_2]^{2+}$, k_2 increases to 5.2 (±0.1) × 10^{-3} $M^{-1}\ s^{-1}$ at pHs 6.3 and 8.2. Within the uncertainty listed in Table I, rate constant k_3 is independent of pH between 6.3 and 8.2. In the case of $Na_2S_2O_4$, the first stage of

(28) Aasa, R.; Vanngard, T. *J. Magn. Reson.* **1975**, *19*, 308–315. Wertz, J. E.; Bolton, J. R. *Electron Spin Resonance. Elementary Theory and Practical Applications*; McGraw-Hill: New York, 1972; pp 462–463.
(29) Lukat, G. S.; Kurtz, D. M., Jr. *Biochemistry* **1985**, *24*, 3464–3472.
(30) Yim, M. B.; Kuo, L. C.; Makinen, M. W. *J. Magn. Reson.* **1982**, *46*, 247–256.
(31) Chrisman, B. L.; Tumolillo, T. A. *Comput. Physics Commun.* **1971**, *2*, 322–330.

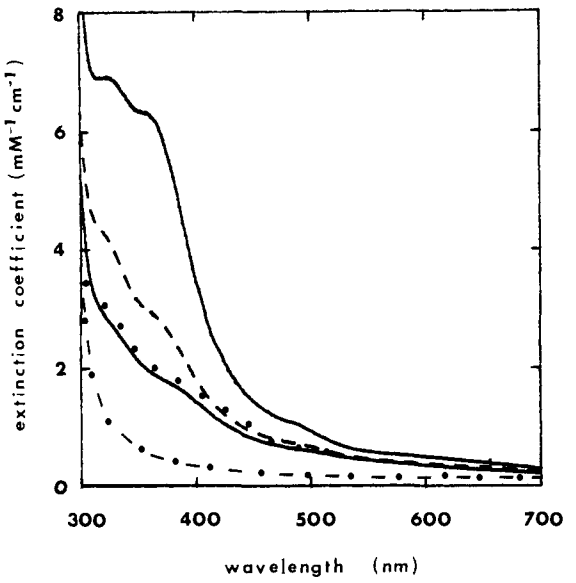

Figure 2. Absorption spectra of the products of reduction of 0.1 mM *P. gouldii* metHr at pH 8.2 (50 mM EPPS), 150 mM Na_2SO_4, 25 °C. Two equivalents of $[Cr(15\text{-ane}N_4)(H_2O)_2]^{2+}$/binuclear iron site was used to reduce metHr to the second- and third-stage products. Key: (—) met; (- - -) first-stage product; (—) (lower curve) second-stage product; (···) second-stage product plus excess N_3^-; (—·—) third-stage product.

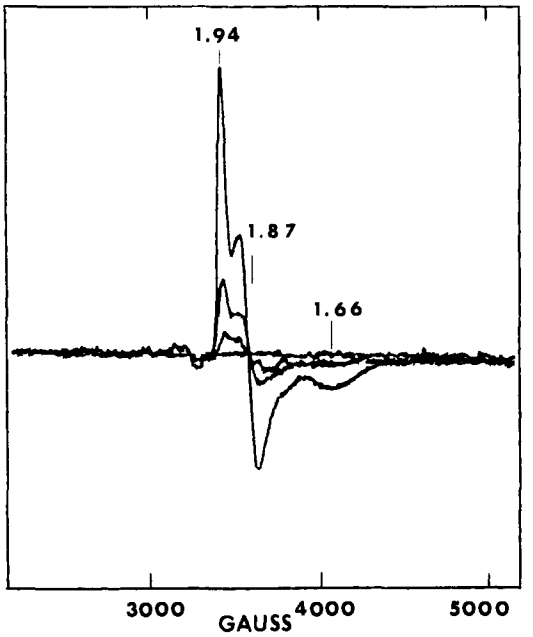

Figure 3. Semi-met EPR signals obtained during reduction of 0.1 mM *P. gouldii* metHr with a 20-fold molar excess of $Na_2S_2O_4$ at pH 7.0 (50 mM HEPES), 150 mM Na_2SO_4, 20 °C. With decreasing intensity spectra are of samples frozen at ~1, 30, 45, and 100 min after mixing. Spectra were obtained at ~4 K. Numbers near the spectra indicate positions of *g* values.

reduction is on the stopped-flow time scale, while the latter two stages can be followed by conventional spectrophotometry. Figure 1 shows that the experimental absorbance vs time data after the first stage of reduction with $Na_2S_2O_4$ are better fit by using two exponentials rather than one exponential. Rate constants k_2 and k_3 are obtained from the two-exponential fit.

The second and third stages of reduction of *P. gouldii* metHr by $[Cr(15\text{-ane}N_4)(D_2O)_2]^{2+}$ in ~95% D_2O were examined at 20 °C and pH 7.0 (50 mM HEPES). No changes in rate constants were observed compared to H_2O; i.e., $k_2 = 3.5\ (\pm 0.4) \times 10^{-3}\ M^{-1}\ s^{-1}$ and $k_3 = 2.0\ (\pm 0.3) \times 10^{-4}\ M^{-1}\ s^{-1}$ in D_2O. The first stage of reduction in H_2O and ~95% D_2O was compared at pH 6.3 (50 mM MES) and 20 °C by using $Fe(EDTA)^{2-}$. Once again no differences were observed; i.e., rate constants of 3.7 (±0.5) $M^{-1}\ s^{-1}$ in H_2O and 3.8 (±0.4) $M^{-1}\ s^{-1}$ in D_2O were found.

Product Identification. For reactions with Cr^{2+}(aq), we consistently found 1.0 ± 0.1 mol of Cr bound/mol of Hr (i.e., per mole of binuclear iron sites) for the first-stage product. For reactions with $[Cr(15\text{-ane}N_4)(H_2O)_2]^{2+}$, we found no Cr bound to Hr at any stage of reduction.

Oxidation levels of the iron sites in both *T. zostericola* and *P. gouldii* Hrs at each stage of reduction were characterized by absorption, EPR, and, for the second and third stages, Mössbauer spectroscopy.

Absorption spectra of the products at all stages of reduction at pH 6.3 are shown in Figure 2 for *P. gouldii* Hr. The first-stage product, irrespective of reductant, is quantitatively at the semi-met oxidation level. Addition of excess N_3^- to the first-stage product results in semi-metHrN_3 (not shown), which can be quantitated with $\epsilon_{470} = 2400\ M^{-1}\ cm^{-1}$.[11] At the end of the first stage 100 ± 5% of the binuclear iron sites can be accounted for as semi-metHrN_3. We used the same method to show that the product of reduction with $Fe(EDTA)^{2-}$ in D_2O is at the semi-met oxidation level. The second-stage product, obtained 30–40 min after mixing, has a spectrum with shoulders at 330 and 380 nm. When N_3^- is added to this product, very little change in absorbance occurs, indicating little or no binding of N_3^-. Exposure of the second-stage product to air results in a spectrum closely resembling that of oxyHr.[32] Quantitative estimates of the concentration of oxyHr from such spectra are complicated by the necessity of accounting for any remaining background absorption of the second-stage product. The third-stage product was identified as deoxyHr by comparison to literature spectra[19] and by conversion to the spectrum of oxyHr upon exposure to air. Reactions carried out at pHs 6.3, 7.0, and 8.2 gave similar absorption spectra at corresponding stages. The absorption spectra of Figure 2 are very similar to those published for the products of the three stages of reduction of *T. zostericola* metHr.[13]

The reduction of metHr can also be followed by EPR spectroscopy. Only the semi-met oxidation level of Hr is known to produce an EPR signal near liquid-helium temperatures with g_{av} ~ 1.84. Figure 3 shows the time course of this EPR signal during reduction of *P. gouldii* metHr at pH 7.0. The most intense signal is produced within the time of mixing and freezing, and its rhombic shape and *g* values identify it as that of $(\text{semi-met})_R$Hr.[16] Double integrations of these signals are consistent with quantitative production (92 ± 20%) of $(\text{semi-met})_R$ at the end of the first stage. The product of the second stage is represented in Figure 3 by the absence of any EPR signal at 100 min. The third-stage product also has no EPR signal, consistent with its identification as deoxyHr. The same EPR signal disappears within 15 min at pH 6.3 and within 30 min at pH 8.2,[32] consistent with the higher value of k_2 at these pHs, mentioned above. Thus, the second stage is characterized by disappearance of the $(\text{semi-met})_R$ EPR signal. In the presence of *excess* reducing agent, no change in EPR line shape occurs during this disappearance.

The preceding observations also apply to the EPR time course during reduction of *T. zostericola* metHr (Figure 4a). The $(\text{semi-met})_R$ EPR signal is produced quantitatively (95 ± 15%) within 30 s after addition of reductant. At ~40 min, no EPR signal is observed and no change in EPR line shape is observed throughout the time course. Figure 4b shows the signals resulting when excess N_3^- is added to each EPR time-course sample immediately prior to freezing. The *g* values (1.92, 1.82, 1.5) and line shape are identical with those previously published for *T. zostericola* semi-metHrN_3.[16] Figure 4 shows that the semi-met EPR signal detected during the course of reduction can be quantitatively converted to that of semi-metHrN_3. In addition, a gradual increase in a signal at $g \sim 13$ can be seen in Figure 4b. This signal has previously been shown to be due to deoxyHrN_3.[10]

In contrast to the case with excess reductant, a change in EPR line shape with time *is* observed when only one reducing equivalent

(32) Pearce, L. L. Ph.D. Thesis, Iowa State University, 1986.

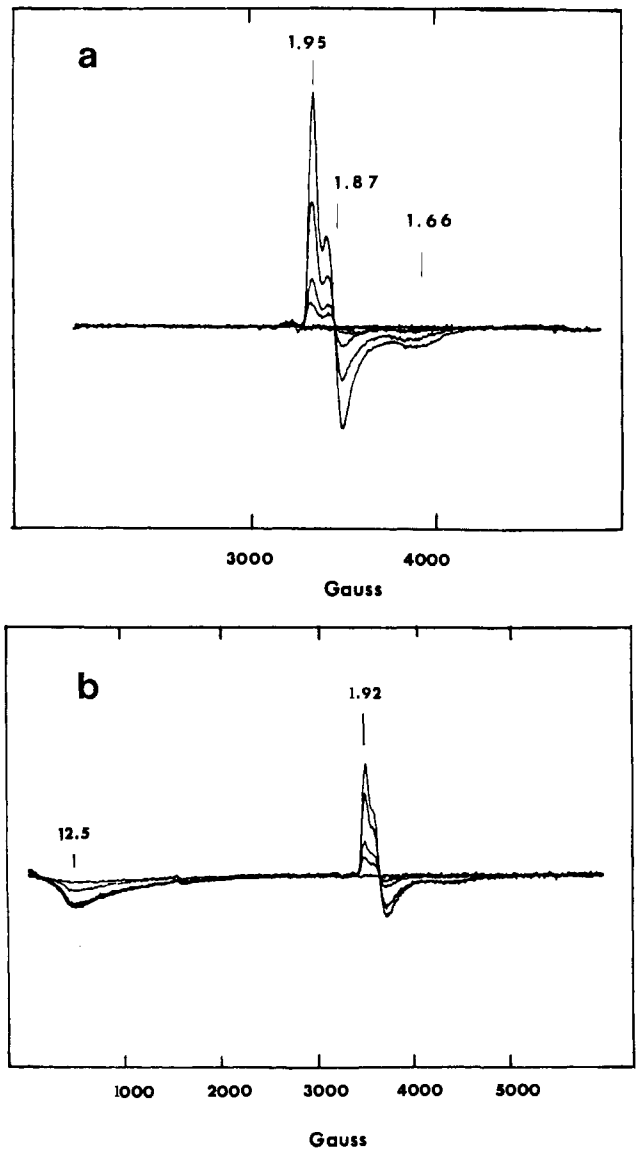

Figure 4. EPR spectra obtained at ~4 K during reduction of 0.1 mM *T. zostericola* metHr at pH 6.3 (50 mM MES), 150 mM Na_2SO_4, 25 °C, with a 20-fold molar excess of $Na_2S_2O_4$. Numbers near spectra indicate positions of *g* values. (a) With decreasing intensity, spectra were obtained at ~0.5, 10, 20, 30, and 40 min after mixing. (b) NaN_3 to 50 mM was added immediately prior to freezing of each sample; with decreasing intensity at $g = 1.92$, spectra were obtained at ~1, 11, 21, 31, and 41 min after mixing.

is used to produce *P. gouldii* $(semi\text{-}met)_R$Hr. Figure 5 shows these changes when 1 equiv of $Cr^{2+}(aq)$ per binuclear iron site is used to reduce *P. gouldii* metHr. The most prominent change is the development of a well-resolved feature at $g = 1.66$. This development, which is equally well observable when using 1 equiv of $[Cr(15\text{-}aneN_4)(H_2O)_2]^{2+}$,[32] occurs on the time scale of the second stage of reduction.

^{57}Fe Mössbauer spectroscopy has previously been shown to be capable of distinguishing deoxy, oxy, met, and semi-met oxidation levels of the iron site in Hr.[1,22,33,34] A Mössbauer spectrum of a sample ~4.5 mM in *T. zostericola* Hr is shown in Figure 6. This sample was frozen 40 min after addition of 1.5 equiv of

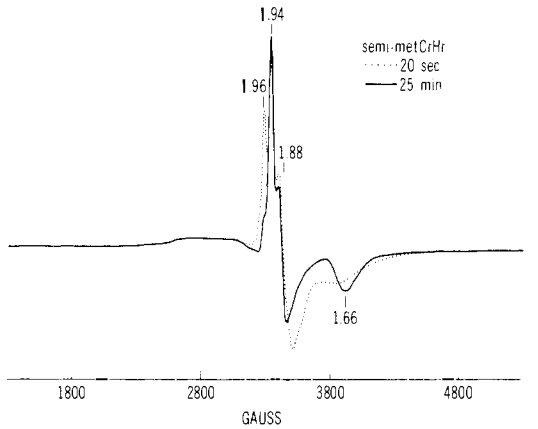

Figure 5. Semi-met EPR signals obtained after reduction of 1.0 mM *P. gouldii* metHr with 1 equiv of $Cr^{2+}(aq)$ at pH 7.0 (50 mM HEPES), 150 mM Na_2SO_4. Solutions were incubated for the indicated times at 20 °C. Spectra were obtained at ~4 K. Numbers near the spectra indicate positions of *g* values. No further changes in EPR line shape occur for at least 24 h. The broad feature near 2800 G is due to Cr(III).

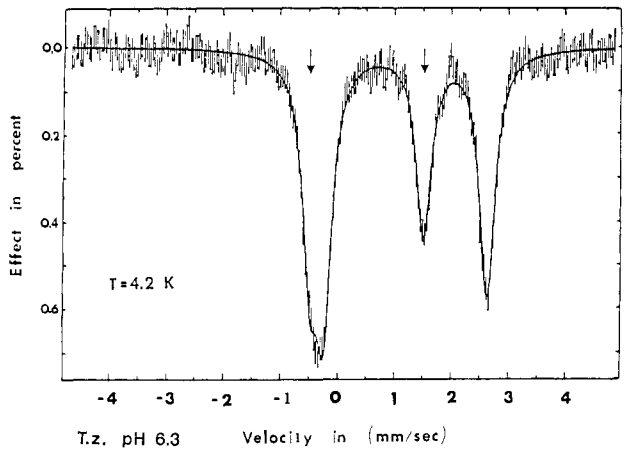

Figure 6. ^{57}Fe Mössbauer spectrum of the second-stage product during reduction of 4.5 mM *T. zostericola* metHr using 1.5 equiv. of $[Cr(15\text{-}aneN_4)(H_2O)_2]^{2+}$ and freezing 40 min after incubation at 25 °C, pH 6.3, 150 mM Na_2SO_4. Spectrum obtained at 4.2 K in a field of 2.2 kG applied perpendicular to the direction of the γ-radiation. The solid curves represent least-squares fits with two pairs of Lorentzians as described in the text. Arrows indicate position of minor doublet.

$[Cr(15\text{-}aneN_4)(H_2O)_2]^{2+}$ and incubation at 25 °C. At this reaction time no EPR signals were seen in samples prepared under comparable conditions (also, cf. Figure 4a). Thus, the spectrum in Figure 6 should be representative of the second-stage product. There is no evidence for magnetic hyperfine splitting or broadening in spectra taken in a 2.2-kG field, at either 4.2 or 1.8 K, consistent with the absence of any Kramers' doublets in this sample. The three features in this spectrum can be attributed to two overlapping quadrupole doublets. The more intense doublet with ~60% of the total area, isomer shift, δ_{Fe}, of 1.15 mm/s, and quadrupole splitting, ΔE_Q, of 2.94 mm/s has parameters close to those we have measured separately for *T. zostericola* deoxyHr (δ_{Fe} (ΔE_Q) (mm/s) of 1.20 (2.83) at 4.2 K). We, therefore, attribute this doublet to a high-spin ferrous center. The remaining doublet in Figure 6 (indicated by arrows) with ~40% of the total area and δ_{Fe} (ΔE_Q) (mm/s) of 0.60 (1.84) has parameters consistent with those of a high-spin ferric center. However, these parameters are somewhat different from those we have measured separately for *T. zostericola* metHr (δ_{Fe} (ΔE_Q) (mm/s) of 0.48 (1.62) at 4.2 K).

Figure 7 shows the Mössbauer spectrum of a sample of *P. gouldii* Hr prepared by reducing ~5 mM metHr at pH 6.3 with a 10-fold molar excess of $Na_2S_2O_4$ and incubating for 15 min at 25 °C. No EPR signal is observed for this sample, consistent with the EPR time course at this pH. Spectra obtained at 4.2 K in

(33) (a) Kurtz, D. M., Jr.; Sage, J. T.; Hendrich, M.; Debrunner, P. G.; Lukat, G. S. *J. Biol. Chem.* **1983**, *258*, 2115–2117. (b) Lukat, G. S.; Kurtz, D. M., Jr.; Shiemke, A. K.; Loehr, T. M.; Sanders-Loehr, J. *Biochemistry* **1984**, *23*, 6416–6422.

(34) Okamura, M. Y.; Klotz, I. M.; Johnson, C. E.; Winter, M. R. C.; Williams, R. J. P. *Biochemistry* **1969**, *8*, 1951–1958. Garbett, K.; Johnson, C. E.; Klotz, I. M.; Okamura, M. Y.; Williams, R. J. P. *Arch. Biochem. Biophys.* **1971**, *142*, 574–583.

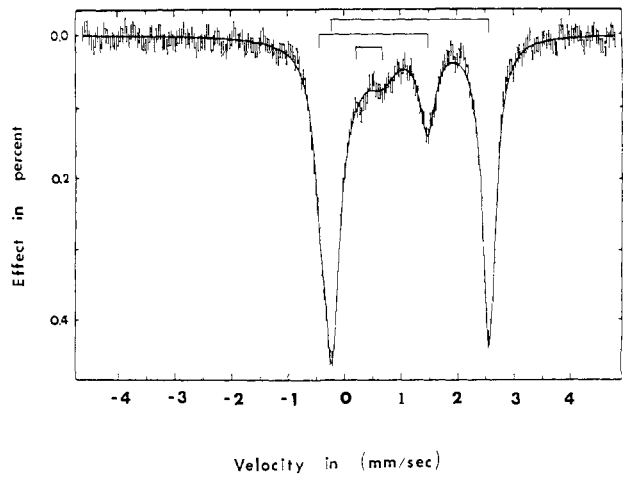

Figure 7. ^{57}Fe Mössbauer spectrum of the second-stage product during reduction of 5 mM *P. gouldii* metHr using a 10-fold molar excess of $Na_2S_2O_4$ and freezing 15 min after incubation at 25 °C, pH 6.3 (50 mM MES), 150 mM Na_2SO_4. Spectrum obtained at 100 K. The solid curves represent least-squares fits to three pairs of Lorentzians as described in the text. Brackets indicate positions of the quadrupole doublets.

fields of 2.2 kG show no significant difference from the 100 K spectrum of Figure 7 and give further evidence for the absence of a semi-met species. Lorentzian fits of these spectra indicate the presence of three quadrupole doublets, which are marked by brackets in Figure 7. The main doublet accounts for 68% of the total area and has parameters δ_{Fe} (ΔE_Q) (mm/s) of 1.18 (2.77) at 100 K. Within experimental uncertainty these values are the same as those published for *P. gouldii* deoxyHr, viz. 1.19 (2.81) at 77 K.[34] The brackets in Figure 7 indicate two other quadrupole doublets accounting for 22% and 10% of the total area with parameters δ_{Fe} (ΔE_Q) (mm/s) of 0.53 (1.89) and 0.47 (0.47), respectively. Both sets of parameters are characteristic of high-spin ferric centers, but both differ from the values, 0.47 (1.62), reported for *P. gouldii* metHr at 110 K.[33a,34] A sample of *P. gouldii* metHr at pH 8.2, which had been reduced with 2 equiv of $[Cr(15\text{-}aneN_4)(H_2O)_2]^{2+}$ and frozen after 30-min incubation at 25 °C, showed a Mössbauer spectrum very similar to that of Figure 7.[32] Attempts to fit the minor intensities in these spectra to the Mössbauer spectrum of oxyHr were unsuccessful.

The power saturation behavior of the EPR signal of the first-stage product, (semi-met)$_R$Hr, was compared to those of two other derivatives, semi-metHrN_3 and (μ-S^{2-})semi-metHr. For relaxation by an Orbach process, the EPR half-saturation power, $P_{1/2}$, as a function of absolute temperature, T, has been well-fitted in other systems[30,35] at all but the lowest temperatures by

$$\ln P_{1/2} = \ln A - \Delta/kT$$

where k is the Boltzmann constant and A is a constant characteristic of the particular system. The value of Δ is a measure of the energy separation between the ground and first excited states. Plots of ln $P_{1/2}$ (mW) vs $1/T$ for (semi-met)$_R$Hr, semi-metHrN_3, and (μ-S^{2-})semi-metHr are shown in Figure 8. Least-squares analyses of the linear portions of each plot generated the slopes, Δ/k, of the lines shown in Figure 8. Within experimental uncertainty, the points for both (semi-met)$_R$Hr and semi-metHrN_3 lie on the same line, while those for (μ-S^{2-})semi-metHr lie on a different line. The values of Δ determined from these plots are 45 ± 3 cm^{-1} for (semi-met)$_R$Hr and semi-metHrN_3 and 86 ± 4 cm^{-1} for (μ-S^{2-})semi-metHr.

Discussion

The results presented above establish for the first time the following characteristics about reduction of the iron sites in octameric metHrs: (i) Stages 2 and 3, observed during reduction

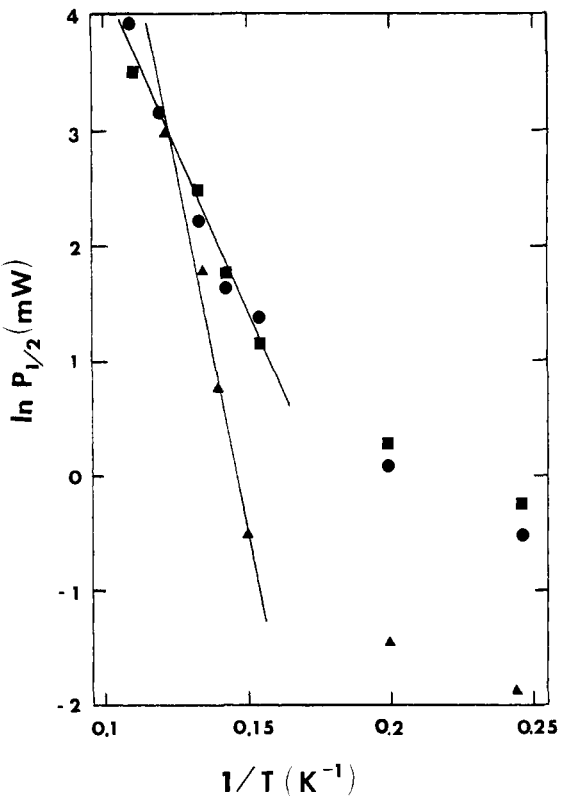

Figure 8. Dependences of the EPR half-saturation powers, $P_{1/2}$, on absolute temperature for various derivatives of *P. gouldii* Hr. Key: (■) semi-metHrN_3; (●) (semi-met)$_R$Hr; (▲) (μ-S^{2-})semi-metHr. Procedures for obtaining these data are described in the Experimental Section.

of *P. gouldii* metHr, have rate constants and absorption spectra very similar to those previously published for *T. zostericola* Hr.[13] (ii) The extent of antiferromagnetic coupling in the first-stage product, (semi-met)$_R$Hr, is ~5 times lower than that in metHr. (iii) The second-stage product consists of a mixture of deoxy and met oxidation levels; the latter we label met′ because of its inability to bind N_3^- and its unusual Mössbauer parameters. (iv) With an excess of reducing agent, the second-stage product contains ~70% of the iron sites at the deoxy level. (v) There are no detectable effects of D_2O on the rates of reduction.

For reduction of *P. gouldii* metHr by $Na_2S_2O_4$, the values of k_2 and k_3 are 2–5 times those previously obtained by other workers.[19] One possible reason for these differences is our use of a nonlinear least-squares algorithm, which fits the absorbance vs time data to a sum of exponentials, rather than the use of semilog plots of $A_t - A_\infty$ vs time. Further support for the correctness of our values for k_2 and k_3 is that very similar values are obtained with three different reducing agents (Table I). Although we detect chromium bound to Hr (presumably as Cr(III)) only when Cr^{2+}(aq) is used as reductant, the rate constants for the second and third stages do not reflect any obvious sensitivity to the presence or absence of bound chromium.

The use of EPR and Mössbauer spectroscopies in conjunction with absorbance changes has given us new insight into the nature of the second-stage product. The lack of an EPR signal at the end of this stage (Figures 3 and 4) rules out the presence of any iron sites at the semi-met oxidation level. The mixture of deoxy and met oxidation levels in the second-stage product, as established by Mössbauer spectroscopy (Figures 6 and 7), is consistent with the occurrence of disproportionation of (semi-met)$_R$Hr during the second stage. Disproportionation has previously been shown to occur without excess reducing agent for *T. zostericola* (semi-met)$_R$Hr and to a lesser extent for *P. gouldii* (semi-met)$_R$Hr.[11]

Armstrong et al.[13] found that 12 reducing equivalents/octamer was consumed during reduction of *T. zostericola* metHr to the second-stage product, which in light of our results would translate to 75% deoxy. We observe ~60% deoxy in the second-stage

(35) Rutter, R.; Hager, L. P.; Dhonau, H.; Hendrich, M.; Valentine, M.; Debrunner, P. *Biochemistry* **1984**, *23*, 6809–6816.

product by Mössbauer spectroscopy of *T. zostericola* Hr (Figure 6). We attribute this difference to our use of 1.5 reducing equivalents/binuclear site for this Mössbauer sample vs a 5-fold molar excess per binuclear site of reducing equivalents used by Armstrong et al. As shown in Figure 7, the use of a 10-fold molar excess of $Na_2S_2O_4$ over *P. gouldii* metHr leads to ~70% deoxy in the second-stage product. The greater proportions of deoxy over met, which are observed in the second-stage products of both *P. gouldii* and *T. zostericola* Hrs, suggest that, in addition to disproportionation, direct reduction of the semi-met oxidation level occurs during the second stage.

^{1}H NMR studies by Maroney et al.[7] have shown that the magnitude of antiferromagnetic coupling in several semi-metHrX complexes ($J \sim -20$ cm^{-1}) and in (μ-S^{2-})semi-metHr ($J \sim -30$ cm^{-1}) is significantly reduced compared to that of the corresponding metHr complexes ($J \sim -100$ cm^{-1}). ^{1}H NMR spectra of the first-stage product, (semi-met)$_R$Hr, have so far been uninterpretable in this regard. We, therefore, turned to EPR power saturation measurements of (semi-met)$_R$Hr to gain insight into the magnitude of J.[36] The power saturation behaviors of the EPR spectra of semi-metHrN$_3$ and (μ-S^{2-})semi-metHr served as "controls" for that of (semi-met)$_R$Hr. These measurements result in values of Δ, the difference in energy between the ground and first excited spin states. For an antiferromagnetically coupled [Fe(II),Fe(III)] system with ground spin state $S = {}^1/_2$, Δ is a function of both the coupling constant, J, and the zero-field splitting energy, D. If $|D| \ll -J$, then $\Delta \simeq -3J$.[37] Assumption of these relationships and use of the values of Δ determined from our EPR power saturation measurements (Figure 8) lead to values of $J \sim -15$ cm^{-1} for both (semi-met)$_R$Hr and semi-metHrN$_3$ and ~ -30 cm^{-1} for (μ-S^{2-})semi-metHr. These values are in very good agreement with those determined from the NMR studies, lending support to our analysis of the EPR power saturation data.

One possible explanation for the decreased extent of antiferromagnetic coupling in (semi-met)$_R$Hr compared to that in metHr is protonation of the μ-oxo bridge between the iron atoms. This explanation is consistent with the magnitudes of antiferromagnetic coupling in synthetic diiron models of the Hr site containing μ-oxo vs μ-hydroxo bridges at Fe(III),Fe(III) and Fe(II),Fe(II) oxidation levels.[3-5] However, no such information is yet available for mixed-valence Fe(II),Fe(III) synthetic models. As noted above, an ~3-fold decrease in extent of antiferromagnetic coupling is observed upon reduction of (μ-S^{2-})met- to (μ-S^{2-})semi-metHr, and resonance Raman studies indicate no protonation of the μ-sulfido bridge in (μ-S^{2-})semi-metHr.[33b,38] Therefore, we must entertain the possibility that no proton is added to the μ-oxo bridge during reduction of met- to (semi-met)$_R$Hr. Lack of protonation is, in fact, consistent with the absence of a D_2O effect on the rate of the first stage of reduction. Protonation of the μ-oxo bridge could instead occur during the second stage, whose rate, as discussed below, we believe to be conformationally controlled.

The development of a well-resolved feature at $g = 1.66$ in the EPR spectrum of (semi-met)$_R$Hr (Figure 5) is characteristic of a change toward a (semi-met)$_O$-type conformation.[11] Similar changes in EPR line shape have been observed previously during disproportionation of *T. zostericola* (semi-met)$_R$Hr.[16] This development occurs on the time scale of the second stage of reduction when stoichiometric amounts of reductant are used. In contrast, only the (semi-met)$_R$ EPR spectrum is observable when excesses of reductant are used (Figures 3 and 4). These results suggest that a conformational change of the type (semi-met)$_R$ → (semi-met)$_O$ may be the rate-limiting step of the second stage of reduction. (Semi-met)$_O$Hr is known to be much more rapidly reduced to deoxyHr than is (semi-met)$_R$Hr.[11]

The results of this study combined with those from previous studies can be rationalized in the context of Scheme I.

Scheme I

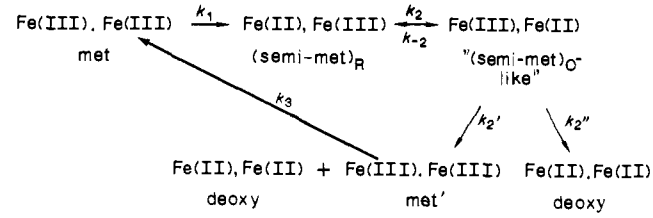

A novel premise implicit in Scheme I is that only the iron atom closer to the outer surface of each subunit in the octamer is directly reduced by "outer-sphere" reducing agents. This atom is labeled Fe1 in the structure shown in the introduction.[2] Thus, the first-stage product, (semi-met)$_R$Hr, would have Fe1 reduced. NMR studies have shown previously that Fe1 is the reduced iron atom in semi-metHrN$_3$.[7] The rate-determining step of the second stage is proposed to involve a (semi-met)$_R$ → "(semi-met)$_O$-like" conformational change.[39] In Scheme I this change is depicted as accompanied by reversal of the oxidation states within each iron site such that Fe1 becomes reoxidized. Only at this point can further reduction by external agents occur. Thus, the (semi-met)$_O$-like species can undergo either a direct reduction to the deoxy level by inorganic reducing agent or disproportionation to met' and deoxy levels. These two transformations are labeled k_2'' and k_2', respectively, in Scheme I, and both are proposed to occur rapidly compared to the k_2 step. According to Scheme I, the relative rates of direct reduction vs disproportionation determine the proportions of deoxy and met oxidation levels in the second-stage product.

Disproportionation of the (semi-met)$_O$-like species could occur intermolecularly by reaction either with the remaining (semi-met)$_R$Hr or with itself if electron exchange within the binuclear iron site is sufficiently rapid. In the latter case, the (semi-met)$_R$ → "(semi-met)$_O$-like" transformation might be better described as a change from slow to fast electron exchange within the binuclear iron site. However, this latter description can also be used to support intramolecular disproportionation, which was previously proposed by Harrington and Wilkins.[41] The Hr octamer consists of two rings of four subunits, with the rings in a face-to-face association. This association results in a face-to-face orientation of the corresponding binuclear iron sites, with the closest intersubunit Fe···Fe distance within the octamer being between Fe2 atoms (cf. structure in the introduction). This distance is reduced to ~18 Å if measured between imidazole edges of His-25 residues.[42] Whether intra- or intermolecular, however, the disproportionation, like the direct reduction, is apparently conformationally controlled. We propose that the conformational change is accompanied by electron exchange between the two iron atoms of each binuclear site.

Insight into a possible origin of this conformational change can be gleaned from considerations of the synthetic models for the diiron site of Hr. The model complexes show that either protonation of the μ-oxo bridge[4] or protonation of the bridge plus reduction[5] should, in the absence of other constraints, lead to a 0.2–0.3-Å lengthening of the Fe1–Fe2 distance. Both reduction and protonation of the μ-oxo bridge may occur during transformation of metHr to the "(semi-met)$_O$-like" species. These considerations raise the possibility that the conformational change

(36) We use the isotropic spin-exchange Hamiltonian, $\hat{H} = -2J\hat{S}_1 \cdot \hat{S}_2$. With this sign convention, $J < 0$ indicates antiferromagnetic coupling.

(37) Gayda, J.; Gibson, J. F.; Cammack, R.; Hall, D. O.; Mullinger, R. *Biochim. Biophys. Acta* **1976**, *434*, 154–163.

(38) Freier, S. M.; Duff, L. L.; Van Duyne, R. P.; Klotz, I. M. *Biochemistry* **1979**, *18*, 5372–5377.

(39) The (semi-met)$_{R,O}$ transformation has previously been formulated as an equilibrium, which, in the case of *T. zostericola* octameric Hr, lies almost completely toward (semi-met)$_O$.[40] However, an equilibration during the k_2 step is not absolutely required for our scheme to explain the observed kinetics. According to our proposed scheme, the "(semi-met)$_O$-like" species can be produced only as a steady-state intermediate. Therefore, we are unable to ascertain whether or not it is identical with (semi-met)$_O$Hr.

(40) Armstrong, F. A.; Harrington, P. C.; Wilkins, R. G. *J. Inorg. Biochem.* **1983**, *18*, 83–91.

(41) Harrington, P. C.; Wilkins, R. G. *J. Am. Chem. Soc.* **1981**, *103*, 1550–1556.

(42) This measurement was made on an Evans & Sutherland Picture System 300 equipped with the MOGLI software package. Coordinates used for *Themiste dyscritum* Hr were those deposited with the Brookhaven Protein Data Bank.

during the second stage of reduction represents adjustments of the surrounding protein necessary to accommodate a longer Fe1-Fe2 distance. We note that difference electron density maps show a longer Fe1-Fe2 distance in deoxy- than in metHr.[8] This proposal is consistent with our earlier suggestion[7] that alteration of the net charge on the binuclear cluster requires adjustments by the surrounding protein.

The third stage, labeled k_3 in Scheme I, is proposed to be the transformation of met′ to met, after which "normal" reduction kinetics resume. The exact nature of the difference between met and met′ is unclear. The preceding discussion suggests a longer Fe1-Fe2 distance in met′ than in met. Another possibility is that met′ has the sixth coordination position on Fe2 occupied by OH^-. Occupancy of this coordination site in met′ would explain the inability of N_3^- to significantly perturb the absorption spectrum of the second-stage product. The rate-determining step for the third stage would then be dissociation of OH^- from Fe2. This proposal is consistent with the kinetics of reduction of the anion adducts, metHrX. Reductions of metHrX are uniphasic, with the rate-determining step being dissociation of X^-.[43] Also, the rate of reduction of metHrOH has been reported to be dependent on conversion to metHr.[44]

Our scheme unifies the kinetics of reduction of octameric Hrs from *T. zostericola* and *P. gouldii* and in addition satisfactorily explains many chemical and physical properties of these two proteins determined in this study as well as in many previous studies. We note that monomeric metmyoHr from *T. zostericola* has reduction kinetics based on absorbance changes, which are quite similar to those of the octameric Hrs.[45] A scheme somewhat different from Scheme I was proposed to explain the kinetics for myoHr, but on the basis of available data, Scheme I seems equally applicable.[46] The apparent physiological reducing agent for metHr, namely, cytochrome b_5,[18] is an "outer-sphere" reagent, and, therefore, is also expected to function according to Scheme I. The implications of our results for the reduction of metHr in vivo will be discussed elsewhere.[47]

Acknowledgment. This work has been supported by grants from the National Institutes of Health (D.M.K., GM 37851; P.G.D., GM 16406).

(43) Olivas, E.; deWaal, J. A.; Wilkins, R. G. *J. Inorg. Biochem.* **1979**, *11*, 205-212.

(44) Bradič, Z.; Wilkins, R. G. *Biochemistry* **1983**, *22*, 5396-5401.

(45) Armstrong, G. D.; Sykes, A. G. *Inorg. Chem.* **1986**, *25*, 3725-3729.

(46) From comparisons of the published absorption spectral time courses,[13,45] it appears that, for myoHr, direct reduction competes relatively effectively with disproportionation during the second stage.

(47) Utecht, R. E.; Kurtz, D. M., Jr., submitted for publication in *Biochim. Biophys. Acta.*

Crown Ether-Cation Decomplexation Mechanics. ^{23}Na NMR Studies of the Sodium Cation Complexes with Dibenzo-24-crown-8 and Dibenzo-18-crown-6 in Nitromethane and Acetonitrile

Alfred Delville,† Harald D. H. Stöver, and Christian Detellier*

Contribution from the Ottawa-Carleton Chemistry Institute, Ottawa University Campus, Ottawa, Ontario K1N 9B4, Canada. *Received February 17, 1987*

Abstract: The mechanisms and the activation parameters of decomplexation have been determined by ^{23}Na NMR for dibenzo-24-crown-8 (DB24C8)-$NaPF_6$ in nitromethane, dibenzo-18-crown-6 (DB18C6)-NaX in acetonitrile (X = BF_4^-, BPh_4^-), and DB18C6-NaY in nitromethane (Y = PF_6^-, BPh_4^-). For DB24C8-$NaPF_6$ in nitromethane, the decomplexation follows a bimolecular exchange mechanism for $[Na^+]_T > 2 \times 10^{-3}$ M, characterized by $\Delta H^\ddagger = 30 \pm 2$ kJ mol^{-1} and $\Delta S^\ddagger = -37 \pm 10$ J mol^{-1} K^{-1}. At lower sodium concentrations, the mechanism is predominantly unimolecular with $\Delta G^\ddagger_{300} \sim 63$ kJ mol^{-1}. For Na^+-DB18C6 in acetonitrile, the mechanism is purely unimolecular with $\Delta H^\ddagger = 40 \pm 2$ kJ mol^{-1} and $\Delta S^\ddagger = -44 \pm 8$ J mol^{-1} K^{-1}. In nitromethane, the bimolecular exchange mechanism is in competition with the unimolecular one. The contributions of the two mechanisms have been separated from the observed rate constants: at 300 K, $\Delta G^\ddagger_{bi} = 48 \pm 4$ kJ mol^{-1} and $\Delta G^\ddagger_{uni} = 60 \pm 3$ kJ mol^{-1}. The activation parameters have been determined for the unimolecular decomplexation mechanism: $\Delta H^\ddagger = 37 \pm 3$ kJ mol^{-1} and $\Delta S^\ddagger = -78 \pm 8$ J mol^{-1} K^{-1}. The comparison with literature data showed that the unimolecular decomplexation mechanism is favored in high-donicity solvents, despite a higher activation enthalpy, which is compensated by a higher activation entropy. It is suggested that the unimolecular decomplexation of Na^+-DB18C6 involves a desolvation step accompanying conformational changes.

Molecular recognition phenomena are being studied at higher and higher levels of complexity. The design of host molecules incorporating specific characteristics has led to high discrimination between guest molecules or cations for the formation of the "host-guest" complex. The crown ethers (chorands, coronands), first synthesized by Pedersen in 1967,[1] opened the way to the cryptands,[2] the spherands,[3] the lariat crown ethers,[4] and channel assemblies.[5] However, the increased sophistication of the relationship between host structure and host-guest complexation lies on mechanisms of complexation-decomplexation which are still poorly understood. This is the case even for basic systems such as the simple coronands. In fact, the crown ether, the cation, the

† Chargé de Recherches FNRS. Permanent address: Institut de Chimie Organique et de Biochimie B6, Université de Liège au Sart-Tilman, B-4000, Liège, Belgium.

(1) Pedersen, C. J. *J. Am. Chem. Soc.* **1967**, *89*, 7017-7036.

(2) Lehn, J. M. *Acc. Chem. Res.* **1978**, *11*, 49-57.

(3) Cram, D. J.; Kaneda, T.; Helgeson, R. C.; Brown, S. B.; Knobler, C. B.; Maverick, E.; Trueblood, K. N. *J. Am. Chem. Soc.* **1985**, *107*, 3645-3657.

(4) Schultz, R. A.; White, B. D.; Dishong, D. M.; Arnold, K. A.; Gokel, G. W. *J. Am. Chem. Soc.* **1985**, *107*, 6659-6668.

(5) (a) Walba, D. M.; Richards, R. M.; Sherwood, S. P.; Haltiwanger, R. C. *J. Am. Chem. Soc.* **1981**, *103*, 6213-6215. (b) Van Beijnen, A. J. M.; Nolte, R. J. M.; Zwikker, J. W.; Drenth, W.; *Recl.: J. R. Neth. Chem. Soc.* **1982**, *101*, 409-410.

0002-7863/87/1509-7293$01.50/0